Surface of Cytochrome *c*: Infrared Spectroscopy of Carboxyl Groups†

Wayne W. Wright, Monique Laberge, and Jane M. Vanderkooi*

Johnson Research Foundation, Department of Biochemistry and Biophysics, School of Medicine, University of Pennsylvania, Philadelphia, Pennsylvania 19104

Received June 27, 1997; Revised Manuscript Received September 18, 1997⊗

ABSTRACT: The carboxylate groups of organic acids give strong absorption in the infrared between ∼1550 and 1650 cm^{-1}. For acetate and chloroacetate derivatives, the infrared (IR) frequency of the carboxylate antisymmetric stretching mode (ν^{a}_{OCO}) is related to the square root of the p*K* of the acid, with a shift of ∼20 cm^{-1} to higher frequency for a p*K* drop in the range 5−3. It follows that ν^{a}_{OCO} may respond to conditions on the protein surface. In this paper, the IR amide I′ and carboxylate absorptions of cytochrome *c* from horse, yeast, and tuna are compared with model compounds such as Val-Glu and microperoxidase-11, the 11 amino acid fragment of horse cytochrome *c* containing the covalently bound heme. For microperoxidase-11, the contribution from all four carboxylates can be accounted for and the 1567 cm^{-1} absorption is assigned to the heme propionates. For the proteins, the carboxylate absorption band is inhomogeneous, i.e., there is a distribution of frequencies. Both the amide I′ and carboxylate bands are sensitive to protein conformation as shown by their different pH, salt, and redox dependence.

Proteins, by virtue of being small and irregular in shape, represent a class of matter that is highly structured, yet having a large surface area. The exact nature of the charged surface of proteins is of interest from several viewpoints: (1) surface charges are critical for ensuring stability and proper folding of the protein, (2) protein electric fields, with a large contribution from the charged residues, modulate the chemistry of the prosthetic groups, (3) the charge distribution ensures specific complexation with cofactors and/or other proteins, and finally (4) electric fields produced by charges on a protein surface can increase reaction rates by directing substrate or cofactor to a particular binding cleft.

For cytochrome *c* (cyt *c*),[1] a monomeric heme electron transfer protein from mitochondria, the importance of the protein surface has been considered from all these aspects. The heme is covalently bound, so protein stability can be examined over the entire pH range without heme loss. Lowering the pH results in a protein folded to a lesser extent and with lower secondary structure stability (Goto et al., 1990a,b). It would appear that there are at least four conformational states of the ferric protein in the pH region ranging between 0.5 and 7.0 (Myer, 1968; Myer & Saturno, 1991). At the same time, changes in the charge distribution brought about by pH are also manifested in the cyt *c* redox chemistry (Moore et al., 1980; Leitch et al., 1984; Rogers et al., 1985). Conversely, changes in the oxidation state of the iron affect the surface properties of cyt *c* as indicated by the tighter binding of the ferric form to membranes and redox partners (Vanderkooi et al., 1973; Vanderkooi & Erecinska, 1974). Finally, electrostatic effects have been proposed to increase rates by promoting the proper orientation of the redox partners (Koppenol & Margoliash, 1982; Matthew et al., 1983; Northrup et al., 1987, 1988, 1990) and maintaining the redox properties (Tiede et al., 1993).

As a probe of surface characteristics, we are using here the infrared (IR) absorbance of carboxyl groups. The vibrations of the carboxyl group give rise to particularly strong absorbencies in the mid-IR range (Lin-Vien et al., 1991). The signal from the carboxylate antisymmetric stretch mode (ν^{a}_{OCO}) has been detected before in cyt *c* (Tonge et al., 1989) and other proteins (Koeppe & Stroud, 1976; Davoodi et al., 1995). Previously, we have shown that, in amino acids, the frequency of this stretch, ν^{a}_{OCO}, decreases with increasing p*K* of the acid (Wright & Vanderkooi, 1997). In qualitative terms, the more stabilized the carboxylate residue is, the higher the ν^{a}_{OCO} and the lower the p*K* for protonation. A relationship between p*K* and frequency has also been established for the carbonyl group of the conjugate acid (Bellamy, 1980) and the OH vibration (Goulden, 1954; Dunn & McDonald, 1969).

In this work, we examine the spectra of model compounds, including acetate derivatives, a small dipeptide (Val-Glu), and microperoxidase 11 (MP-11), the 11 amino acid peptic digest from horse cyt *c*, which retains the covalently bound heme. We then show that the IR absorption of the carboxylate stretch depends upon characteristics of the protein conformation and charge. For reference, the sequences of amino acids in the studied cytochromes, from horse, yeast, and tuna, are given in Table 1.

MATERIALS AND METHODS

Cyt *c* from horse, tuna, and yeast, MP-11, D_2O, DCl, and Val-Glu were obtained from Sigma Chemical Co. (St. Louis, MO). Water was deionized and glass distilled. Other chemicals were of the highest purity commercially obtainable.

A Bruker IFS 66 FTIR spectrometer (Bruker Inc., Brookline, MA) configured with a Globar source, a KBr beam splitter,

† Supported by NIGMS (National Institutes of General Medical Sciences) Grant PO1-GM48130.

* Author to whom correspondance should be addressed. E mail: vanderko@mail.med.upenn.edu.

⊗ Abstract published in *Advance ACS Abstracts,* November 1, 1997.

[1] Abbreviations: cyt *c*, cytochrome *c*; ATR, attenuated total reflectance; FTIR Fourier transform infrared spectroscopy; IR, infrared; MP-11, microperoxidase 11, ν^{a}_{OCO}, frequency of the carboxylate antisymmetric stretching mode; ν^{s}_{OCO}, frequency of the carboxylate symmetric stretching mode; ν_{CO}, frequency of the carbonyl stretching mode; CTAB, cetyl dimethyl ammonium bromide.

S0006-2960(97)01559-6 CCC: $14.00

Table 1: Sequences of Horse (H), Yeast (Y), and Tuna (T) cyt *c*[a]

						1	2	3	4	5	6	7	8	9	10	11	12	13	14	15	16	17	18	19	20
H						G	D	V	E	K	G	K	K	I	F	V	Q	K	C	A	Q	C	H	T	V
Y	T	E	F	K	A	G	S	A	K	K	G	A	T	L	F	K	T	R	C	L	Q	C	H	T	V
T						G	D	V	A	K	G	K	K	T	F	V	Q	K	C	A	Q	C	H	T	V
H						E	K	G	G	K	H	K	T	G	P	N	L	H	G	L	F	G	R	K	T
Y						E	K	G	G	P	H	K	V	G	P	N	L	H	G	I	F	G	R	H	S
T						E	N	G	G	K	H	K	V	G	P	N	L	W	G	L	F	G	R	K	T
H						G	Q	A	P	G	F	T	Y	T	D	A	N	K	N	K	G	I	T	W	K
Y						G	Q	A	E	G	Y	S	Y	T	D	A	N	I	K	K	N	V	L	W	D
T						G	Q	A	E	G	Y	S	Y	T	D	A	N	K	S	K	G	I	V	W	N
H						E	E	T	L	M	E	Y	L	E	N	P	K	K	Y	I	P	G	T	K	M
Y						E	N	N	M	S	E	Y	L	T	N	P	J	K	Y	I	P	G	T	K	M
T						E/N	N/D	T	L	M	E	Y	L	E	N	P	K	K	Y	I	P	G	T	K	M
H						I	F	A	G	I	K	K	K	T	E	R	E	D	L	I	A	Y	L	K	K
Y						A	F	G	G	L	K	K	E	K	D	R	N	D	L	I	T	Y	L	K	K
T						I	F	A	G	I	K	K	K	G	E	R	Q	D	L	V	A	Y	L	K	S
H						A	T	N	E																
Y						A	C	E																	
T						A	T	S																	

[a] Underlined residues form MP-11. Boxed residues are involved in the covalent attachment of the heme. The origin of tuna cyt *c* obtained from the commercial supplier can be either bonito or albacore variety or be a mixture. Where two amino acids are indicated, the first is for bonito.

and a liquid nitrogen-cooled MCT detector was used for all FTIR measurements. The attenuated total internal reflectance (ATR) technique was used for all measurements. A trapezoidal 6-reflection ZnSe crystal (transmission in the region of interest ~35%) with a refractive index of 2.4 was mounted on a ATR accessory cell (Graseby-Specac, Fairfield, CT). MCT detectors are known to be responsible for quantitative spectral errors because their response is often nonlinear, especially at the center burst. To minimize this problem, spectra were acquired with a narrow aperture (2.5−5 mm), which led to a spectral resolution of <0.5 cm^{-1} in the region of interest. The linearity of the response of the MCT was ensured by consistently checking regions of the spectrum where no light should absorb. Spectra were an average of either 64 or 128 interferograms recorded at a resolution of 0.5 cm^{-1}. The acquisition time for each spectrum was ~2 min. A four point apodization function (FWHM relative to resolution = 0.71) was used with the Opus acquisition software. The spectrometer was flushed with dry nitrogen for ~1 h before starting the measurement. However, the contribution of water vapor to the sample and reference changed somewhat over the several hours used to acquire the data for the pH titrations. We have found that the water vapor contribution can be minimized by acquiring the spectra at 0.5 cm^{-1} resolution, then subtracting the water vapor contribution from the region of interest and finally converting the spectra to a final resolution of 2 cm^{-1} using the *Opus* FTIR data treatment software package (Bruker Inc.). Because water vapor lines are narrow (<0.5 cm^{-1}), whereas the lines of interest are wider than 2 cm^{-1}, this procedure helps to reduce the water vapor contribution without degrading the resolution of the sample spectrum.

The temperature of the sample was ambient, i.e., 20−22 °C. The reference was the phosphate buffered D_2O or H_2O solution. The Na salt of phosphate was used, and since a pH range was studied, the stated buffer concentration indicates the phosphate concentration. The protein samples were incubated ~3 h in the buffer at room temperature before measurement. Usually the pD titration was started at the extreme pD (under which conditions the rate of exchange of the amide protons is fast). The pD was changed by adding aliquots of NaOD or DCl directly to the sample in the ATR cell, and the pD was measured in the cell using a model MI-414b microelectrode (Microelectrodes, Inc., Londonderry, NH). The observed pH value was changed to pD by adding 0.4. After the extreme pDs were examined, representative spectra were taken at neutral pD to ascertain that the titration profiles were reversible.

RESULTS

Factors Influencing the OCO Vibrational Frequencies. The IR spectra of acetate and chloroacetates are characterized by strong ν^{a}_{OCO} and ν^{s}_{OCO} absorptions, the former observed between 1500 and 1700 cm^{-1} and the latter occurring at lower frequency, in the 1300−1400 cm^{-1} range. Their frequencies are given in Table 2. With increasing electron withdrawal capacity, achieved by addition of successive electronegative Cl substituents, ν^{a}_{OCO} is shown to increase

Table 2: ν_{OCO} and $\nu_{C=O}$ for Acetate and Its Derivatives[a]

compound	solvent	ν^a_{OCO}	ν^s_{OCO}	$\nu_{C=O}$	p*K*
acetate	D_2O	1562	1417	1709	4.75
	methanol	1580			
	ethanol	1580		1711	
chloroacetate	D_2O	1601	1398	1721	2.85
	methanol	1616			
	ethanol	1616		1732	
dichloroacetate	D_2O	1635	1381	1734	1.48
	methanol	1648			
	ethanol	1646		1738	
trichloroacetate	D_2O	1665	1339		0.7
	methanol	1677			
	ethanol	1678		1752	

[a] p*K*s in H_2O are taken from the Handbook of Chemistry and Physics (Weast & Astle, 1982−1983).

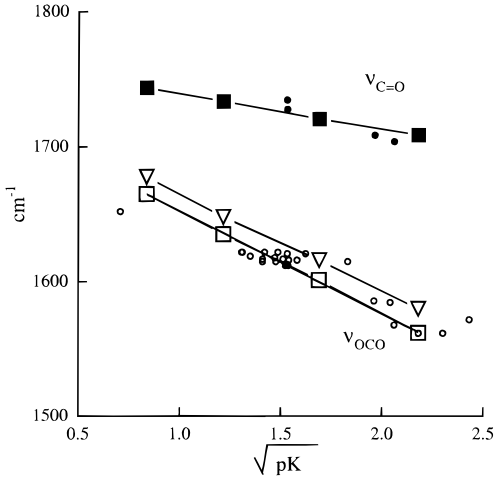

FIGURE 1: Frequency as a function of p*K*. Open symbols are for ν^a_{OCO} of the carboxylate compounds and closed symbols are for $\nu_{C=O}$ of the carboxylic acid. Squares are data for acetates in D_2O and triangles are acetates in ethanol (Table 2). Circles are data from (Wright & Vanderkooi, 1997) for amino and dicarboxylic acids.

as ν^s_{OCO} decreases, while $\nu_{C=O}$ for the conjugate acid increases (Table 2). The p*K* is shown to drop with increasing electron withdrawal capacity, as expected from a relationship between force constant and frequency. In simple cases, the frequency of a vibration can be described by Hooke's Law:

$$\nu = 1/2\pi\sqrt{(k/\mu)} \quad (1)$$

where μ is the reduced atomic mass and k is the force constant. As seen in Figure 1, there is a linear dependence of the frequency with the square root of the p*K* for these compounds. The ν^a_{OCO} frequencies for the acetate derivatives in D_2O are empirically related to p*K* by:

$$\nu^a_{OCO} = -76.2\sqrt{pK + 1730} \quad (2)$$

For acids with p*K*s in the range 3−5, the value of ν^a_{OCO} increases by about 20 cm^{-1}/unit decrease of p*K*. Figure 1 also shows the frequencies previously reported for amino acids and other carboxylic acids (Wright & Vanderkooi, 1997), and these also approximately follow this relationship.

The following relationship was found to hold for $\nu_{C=O}$ (in inverse centimeters) of the conjugate acid, data also given in Table 2:

$$\nu_{C=O} = -25.9\sqrt{pK + 1760} \quad (3)$$

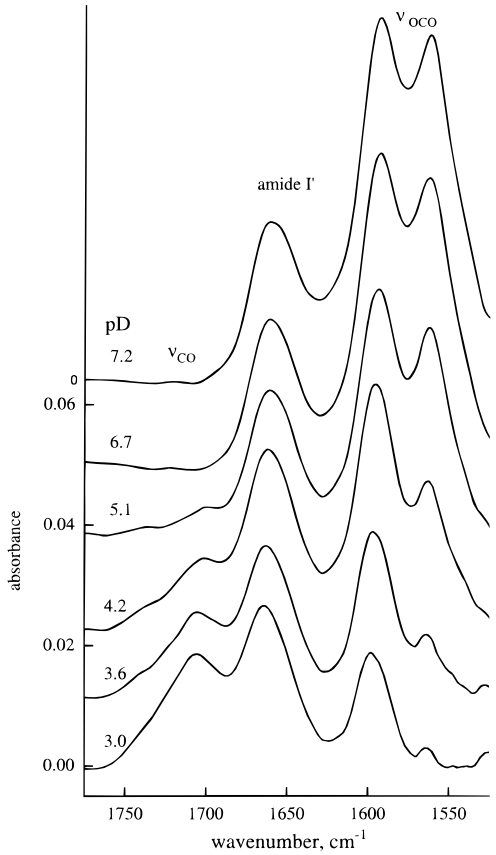

FIGURE 2: Absorption spectra of Val-Glu. The sample was 100 mM in 20 mM phosphate and D_2O at pDs indicated.

Table 3: Frequency (cm^{-1}) for Compounds in D_2O at Neutral pD

		ν^a_{OCO}	
compound	amide I′	α	γ
Glu		1616	1568
Val-Glu	1661	1594	1564
MP-11	1644	1592	1567

This correlation results in an increase of ~6 cm^{-1}/p*K* unit decrease in the same range.

The effective dielectric constant at the surface of a protein is different from that of the protein interior (Simonson & Perahia, 1995). Since all carboxylates are surface groups, we wanted to investigate the vibrational frequency in protic solvents with different dielectric constants. The ν^a_{OCO} frequencies seen in methanol and ethanol were identical (Table 2), in spite of the different dielectric constants of the two solvents (respectively, 32.6 and 24.3). Plots of ν^a_{OCO} versus p*K* yield identical slopes whether the solvent was D_2O, methanol, or ethanol (Table 2 and Figure 1). Hence, there is no simple, direct dielectric effect on the frequency.

IR Spectrum of Val-Glu and MP-11. MP-11 has a terminal Glu, as do horse and tuna cyt *c*s (Table 1). To sort out the relative contributions of its two carboxyl groups, the dipeptide Val-Glu was examined as a function of pD. The spectra are shown in Figure 2 and the frequencies are listed in Table 3. At neutral pD, two peaks observed at 1594 and 1564 cm^{-1} are assigned to the antisymmetric stretches of the two COO groups present. The peak at 1564 cm^{-1} has a higher p*K*, and it is assigned to the γ-COO while the lower peak is attributed to the α-COO.

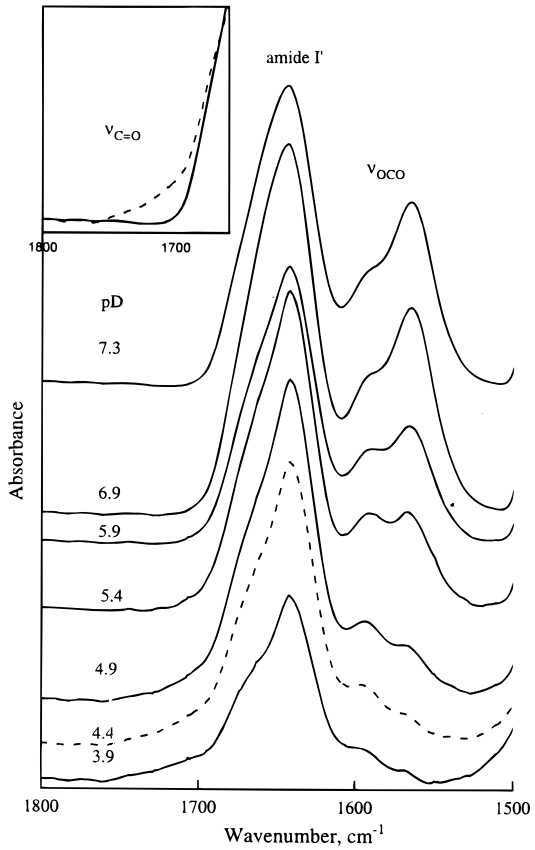

FIGURE 3: Absorption spectra of MP-11 at various pDs. The sample contained 3.5 mM MP-11 in 20 mM phosphate and 1% CTAB in D_2O. pDs are indicated on the figure. (Inset) Amide I′ region for MP-11 at pD 7.3 (solid line) or 4.44 (dotted). Spectra in inset were normalized to give the same maximum absorption.

The IR spectra of MP-11 at different pDs are shown in Figure 3. The large asymmetric peak at 1642 cm^{-1} is assigned to the amide I′ stretch. The peak at 1450 cm^{-1} is a convolution of several types of vibrations, including the amide II′ stretch, as well as contributions from the side groups and possibly from residual HOD (Krimm & Bandekar, 1986). The two peaks at 1567 and 1592 cm^{-1} are attributed to the antisymmetric stretch of the carboxylates; their intensities are observed to decrease as the pH is lowered. At the same time, the $\nu_{C=O}$ contribution, seen at ~1705 cm^{-1} as a broad shoulder on the amide I′ peak, increases. This is clearly seen in the inset of Figure 3 where the amide I′ band region is plotted for MP-11 at pD 7.3 and 4.4.

We therefore assign the peak observed at 1592 cm^{-1} in MP-11 to the α-carboxyl of glutamate. Absorbance versus pD is plotted in Figure 4. Upon the basis of the relative absorption, we can estimate that two carboxyl groups of Glu have p*K*s of 4.7 and 6.9, respectively. The p*K*s of the propionic acids in D_2O are then ~7. The relationship derived above for chloroacetates (i.e., that the carboxyl with a higher frequency stretch has a lower p*K*) also is valid for MP-11 since the peak observed at 1592 cm^{-1} has the lower p*K*.

The amide I′ band also deserves comment. Its frequency maximum is at 1644 cm^{-1} in MP-11 at pD 7.3; this compares with 1642 cm^{-1} reported for N-methylacetamide in D_2O (Diem, 1993). While the undecapeptide may have basically the same fold as these residues have in cyt *c* (Wilson & Ranson, 1977; Laberge et al., 1997), all its residues are nonetheless fully solvated with no secondary structural features. In the Val-Glu dipeptide, the amide group is

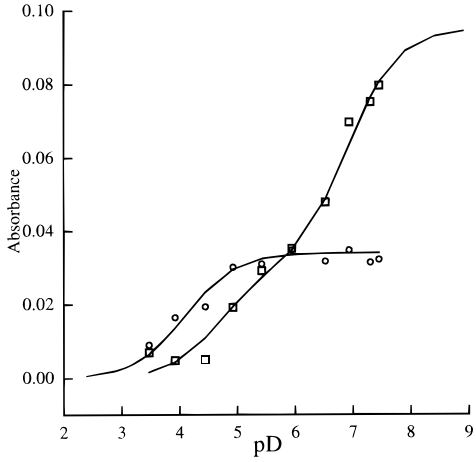

FIGURE 4: Titration curves for MP-11. Conditions given in Figure 3. (○) Absorbance at 1591 cm^{-1}, solid line a simulated titration curve using a Henderson−Hasselbach equation with p*K* 4.1; (□) 1565 cm^{-1}; solid line is a simulated curve with a p*K* of 4.7 and 6.9, with respective amplitude ratio of 1:2.

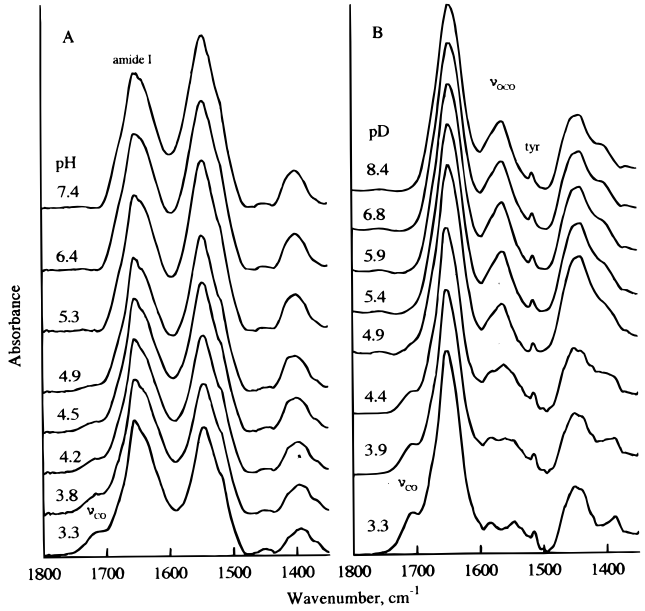

FIGURE 5: Absorption spectra of yeast ferri-cyt *c*. (A) Cyt *c* (5.3 mM), 20 mM $NaPO_4$, and H_2O; (B) 8 mM cyt *c* in 20 mM D_3PO_4. pHs and pDs are indicated on the figure.

adjacent to the positively charged amino terminal residue. The frequency of the amide I′ band which shifts to 1659 cm^{-1} may be affected by the electron-withdrawing nature of this charged residue. However, the story is likely to be more complex than this as a computational approach would indicate (Dwivedi & Krimm, 1984; Krimm & Bandekar, 1986).

pH Titration in H_2O and D_2O for Yeast Cyt c. Since H_2O and D_2O are quite similar and it is well established that the native structure of proteins is retained in D_2O, there was no need to perform a control experiment comparing the IR spectra in H_2O and in D_2O. However, the pH titration of yeast Fe(III) cyt *c* in H_2O can help confirm the assignments for the protein in D_2O. As seen in Figure 5, the amide I band is somewhat broader and more structured than the corresponding peak (i.e., amide I′) in D_2O, but both are asymmetric, indicating that the band is an envelope of several transitions. This is supported by the spectra of horse cyt *c*

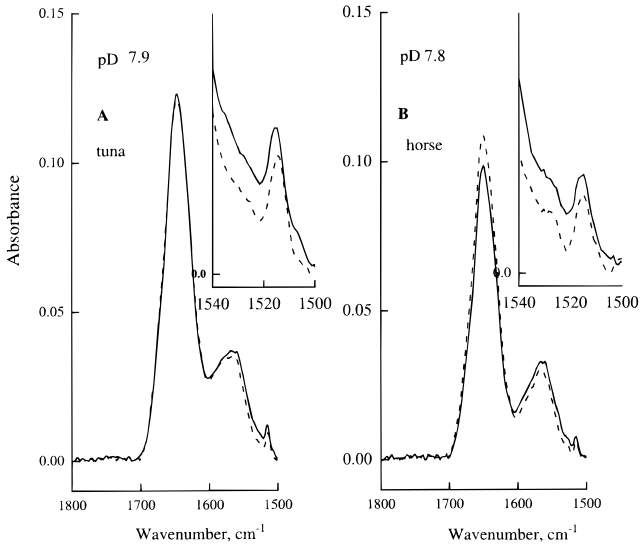

FIGURE 6: Absorption spectra of ferri- (solid line) and ferro- (dotted line) cyt *c*. (A) 4 mM tuna cyt *c*, pD 7.9. (B) Horse cyt *c* (4 mM) at pD 7.8. The buffer was 20 mM PO_4 buffer in D_2O.

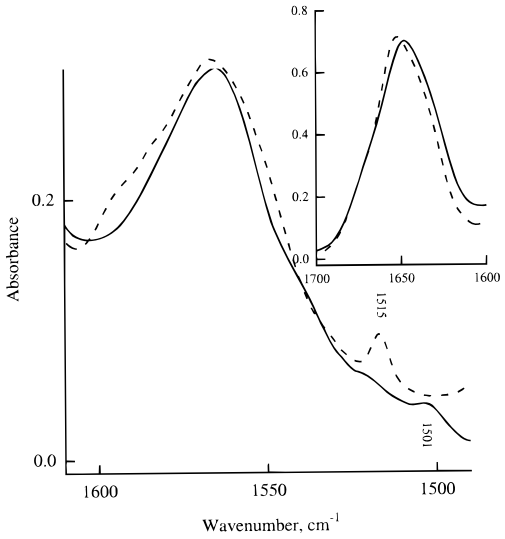

FIGURE 7: Absorption spectra of horse ferri-cyt *c*. The protein was 4 mM at pD 7 (dashed line) and pD 11 (solid line) in D_2O and 1 mM Na PO_4 buffer.

which were fit with up to 7 gaussians (Heimburg & Marsh, 1993). The 1400 cm^{-1} band of ν^s_{OCO} is clearly seen as a peak in H_2O and as a shoulder in D_2O. For both solvents, increasing the acidity causes $\nu_{C=O}$ to appear at ~1720 cm^{-1}. Another constant feature in the cyt *c* spectra for both deuterated and aqueous solution (and not seen in MP-11) is a band at 1515 cm^{-1} observed as a full peak in D_2O and as a shoulder in H_2O. This is assigned to a stretch from Tyr (Chirgadze et al., 1975), and its pronounced intensity is due to that fact that yeast cyt *c* has five Tyr residues (Table 1).

The major difference in the spectra recorded in deuterated and aqueous buffer is the change observed in the amide II band; this band is largely composed of N-H or N-D contributions (Bandekar, 1992). In H_2O (Figure 5A), it overlaps ν^a_{OCO}, and in D_2O, it partially overlaps ν^s_{OCO} (Figure 5B). But even in the aqueous sample, the ν^a_{OCO} contribution is evident when we consider the increased ratio of the 1640 cm^{-1} band to that of the 1560 cm^{-1} at pHs where the carboxyl group becomes deprotonated.

Since in D_2O the ν^a_{OCO} contribution is quite distinct from the amide II′ stretch, deuterated buffer was used in the remaining experiments. As noted in the Materials and Methods, the reversibility of titration curves was used to ascertain that most hydrogens contributing to the amide II band had been exchanged before the experiment started.

IR Spectra of Tuna and Horse Cyt cs. The IR spectra of ferric and ferrous cyt *c* from tuna at pD 7.9 and horse at pD 7.8 are shown in Figures 6. The carboxyl band region is broad for both cytochromes. This suggests *that there is a distribution of carboxyl environments that produce different pKs and frequencies*. The inset shows the Tyr ring stretch, observed at 1515 cm^{-1} for Fe(III) horse cyt *c* and at 1514 cm^{-1} for Fe(II) tuna cyt *c*. At the specified pDs in the presence of buffer, no difference between the ferric and ferrous protein was seen. As presented below, more extreme conditions were required to result in observable differences between the oxidized and reduced proteins.

If we assume that neighboring charged groups have an influence on ν_{OCO}, then the frequency should change at high pH where the lysines are no longer charged. As seen in Figure 7, the carboxyl peak narrows at pH 11, while the 1585 cm^{-1} shoulder definitely vanishes with concomitant narrowing on the low-frequency side. The maximum is then found at 1565 cm^{-1}. This frequency is close to that of a carboxyl fully exposed to solvent, cf. ν^a_{OCO} of acetate in D_2O at neutral pD is observed at 1562 cm^{-1} (Table 1). Since lysine is no longer charged, the narrowing of the spectrum can be interpreted as indicative of loss of charge interactions. There may also be a loss of structure at high pD, as suggested by the change of the amide I′ peak position at 1652 cm^{-1} at pD 7 to 1648 cm^{-1} at pD 11.5 (inset). The axial methionine bond to the iron is broken at high pH, thus lowering the structural integrity of the protein (Gupta & Koening, 1971; Morishima et al., 1977).

Figure 7 also shows that the 1515 cm^{-1} peak disappears at high pH and that a new peak appears at 1501 cm^{-1}. These peak positions and their pD dependence confirm the assignment of the Tyr ring stretch (Goormaghtigh et al., 1994).

Spectra of Horse Heart Cyt c as a Function of pH, Redox, and Salt Concentration. Spectra of horse cyt *c* in two oxidation states are shown as a function of pD in the region from 1500 to 1800 cm^{-1} in Figure 8. Protonation of the carboxyl groups takes place over an extended range, presumably because of charge−charge interactions and pH-dependent changes occurring in the protein. The pD dependence of the spectra for the oxidized and reduced cyt show subtle differences. There is a definite peak at ~1595 cm^{-1} for the ferrous form, which is similar to MP-11, where different populations could be distinguished in the spectra.

The pD-induced changes observed in the spectra also depend upon the salt concentration. Figure 9 shows spectra of horse cyt *c* at two salt concentrations, at 1 and 100 mM phosphate. At high salt, half-protonation of the carboxylates is at about pD 5. At low salt, this value is approximately pD 4 (Figure 9C).

Spectra of Tuna Cyt c as a Function of pH. The IR spectra of cyt *c* from tuna at various pDs are shown in Figure 10. The amide I′ peak is observed at 1648 cm^{-1}. The broad absorption band seen from 1520 to 1600 cm^{-1} in the carboxylate region and the sharp peak observed at 1515 cm^{-1} and assigned to Tyr are clearly discernible. The amide I′ peak observed at high pH is shifted to a maximum at 1645 cm^{-1}.

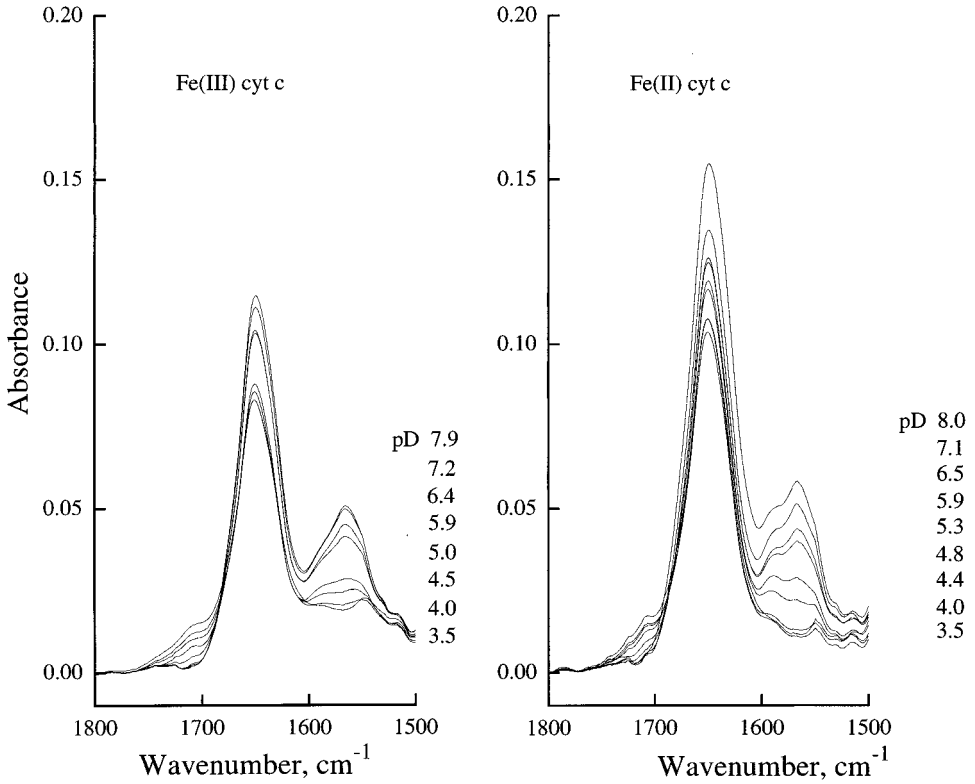

FIGURE 8: pD dependence of the absorption spectrum of 4 mM horse cyt *c*. (Left) Fe(III) cyt *c*; (Right) Fe(II) cyt *c*. The buffer was 20 mM Na PO_4. pDs are indicated on the figure, with the sequence corresponding to the absorbance at ~1565 cm^{-1}.

We comment on features at lowest pD. A peak at about 1540 cm^{-1} is seen in the spectrum at the lowest pH (Figure 10). This peak is also seen at low pH in the horse cyt *c* spectra (Figures 8 and 9A). We cannot make an assignment at this point, but it is in the range of porphyrin pyrrole ring C−N stretches [1547 cm^{-1} in nickel porphin and 1543 cm^{-1} (00) in Ni-OEP] (Ogoshi et al., 1972; Alben, 1978; Kitagawa & Ozaki, 1987). Finally, there is a peak at ~1590 cm^{-1}. The guanidino moiety of Arg shows a stretching frequency in this range (Wright & Vanderkooi, 1997). The proteins each have two Arg (Table 1).

DISCUSSION

Carboxylate Absorption. In this work, our aim was to relate the ν^{a}_{OCO} stretch observed in cyt *c* to conditions of the protein surface. Vibrational frequency is related to bond strength, and both are sensitive to the local electric field. Electric field variations will thus have an influence on both the frequency and the intensity of IR transitions (Liptay, 1974). In the spectra of our model compounds (Table 2), substituents that are electron withdrawing increase the positive charge on the carbon and produce a shift of ν^{a}_{OCO} to higher frequency. In the chloroacetates, this shift is related to p*K* (Figure 1). A shift to higher frequency is also observed in the model compounds for carboxyl groups located near the amino groups. The value of ν^{a}_{OCO} in zwitterionic Gly is 1621 cm^{-1}, as compared with 1562 cm^{-1} for acetate (Wright & Vanderkooi, 1997). In Val-Glu, the α carboxyl vibration is seen at 1594 cm^{-1}. The charged group in Gly is located two bonds away from the carboxyl as compared to a distance of five bonds in Val-Glu.

In the protein, the closest through-bond interactions between positive and negative charges could occur, for instance, in Lys-Glu or Asp-Lys segments. But, if 10 or 11 bonds separate the charges, it is unlikely that through-bond interactions would have any effect. However, because the charged groups are on the surface of the protein, it can be expected that neighboring positively charged groups would be electron withdrawing. For cyt *c* at high pH, where lysine amino groups begin to deprotonate, ν^{a}_{OCO} mostly shifts to lower frequency (Figure 7), consistent with the view that neighboring positively charged residues are affecting the COO^{-} frequencies. The spectra of the carboxylate region in the proteins are not resolved enough to allow identification of individual carboxyls. We believe that this broadening occurs as a result of the presence of other neighboring charged groups which can lie very close to each other, thus, being within charge interaction distance and able to affect one another as well as the monitored carboxylates. Recent theoretical work (Augspurger et al., 1991; Park et al., 1991; Kushkuley & Stavrov, 1996) has conclusively shown that the presence of a point charge significantly shifts vibrational CO frequencies in heme proteins.

At this point, it may be of interest to discuss how the water structure and dielectric properties around the carboxylate group may affect the frequency. For the chloroacetates, ν^{a}_{OCO} is observed at lower frequency in water than in methanol and in ethanol, but little difference is seen between the two alcohol solvents (Table 2). For chlorophyll, ν_{CO} in protic solvents was seen to be independent of solvent dielectric constant, whereas in non-hydrogen-bonding solvents, a dependence upon the solvent dielectric was seen (Koyama et al., 1986; Krawczyk, 1989). Since the solvents used in our study are hydrogen bonding, the lack of dependence upon dielectric may likewise be attributed to the formation of a hydrogen bond. We can point out that when charge effects are "externally" applied (as opposed to a through-bond interaction), as is the case when a charged

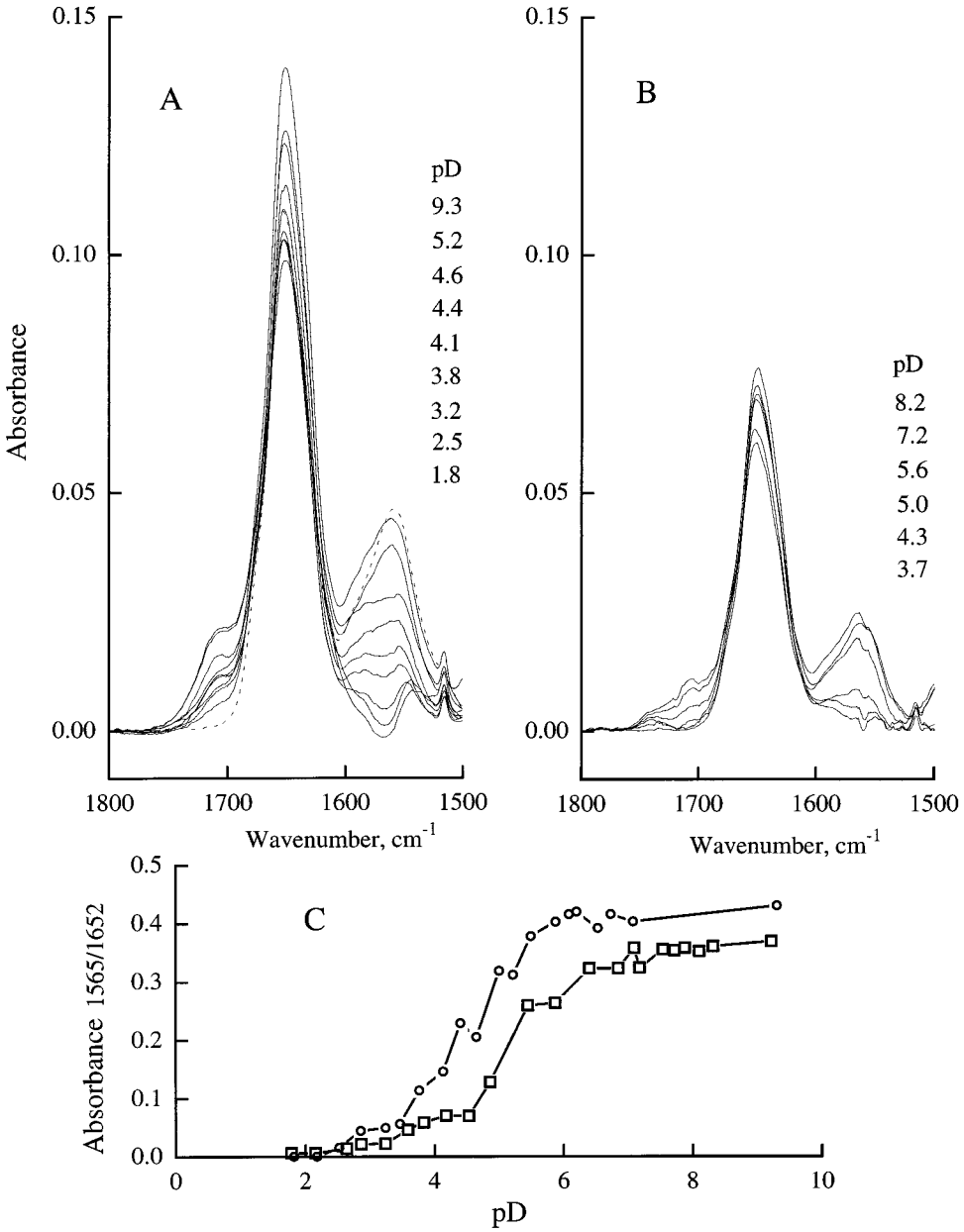

FIGURE 9: pD dependence of horse cyt *c*. The protein was 4 mM. pDs are indicated on the figure, with the sequence corresponding to the absorbance intensity at ~1565 cm^{-1}. (A) PO_4 buffer (100 mM). For clarity, the spectrum at pD 9.3 is shown as a dotted line. (B) PO_4 buffer (1 mM). (C) pH dependence of the ratio of the absorbance of the asymmetric COO^- stretch (1566 cm^{-1})/absorbance of amide I′ (1652 cm^{-1}).

R-group or a point charge is located near the species giving rise to the IR absorption, then the dielectric properties of the intervening solvent may play a role in the shift of the frequency.

For interactions occurring between charged residues on the surface of the protein, we would expect high salt to screen the charges and affect the magnitude of the electric field imposed by the neighboring atoms. This supposition was tested by comparing the pD profiles for the protein acquired at high and low salt concentrations. The protein carboxyl groups more readily accept a proton at high salt concentration than at low salt (Figure 9C). If neighboring positive charges are present, then these charges will be screened at high salt concentration and the protonation p*K* should be very close to that of a free carboxylic acid (for example, 4.75 for acetate), as experimentally observed. High salt may also affect the spectrum by stabilizing the structure, as is well-known. At acid pH and high ionic strength, the α-helices are preserved and the loop region is flexible and partly disordered (Jeng et al., 1990). Lowering the salt concentration reduces the stability of the protein (Jeng & Englander, 1991), and these stability variations may also affect the strength of the amide I′ band as the pD is decreased.

In addition to charge effects, any direct bonding to carboxyl groups will affect the frequency. As noted above, metal ligation shifts the frequency, and we would expect that salt linkages would also result in shifted frequencies. The X-ray structure of yeast cyt *c* (Louie & Brayer, 1990) identifies at least one salt linkage, involving two residues (His 26 and Glu 44), 2.76 Å apart from each other. Modification of salt linkages may be responsible for some of the pH-dependent changes observed in the band intensities and positions of all the spectra.

Redox Properties, Salt Effects, and Protein Stability. Changing the oxidation state of the heme iron changes the charge within the protein, and a question was whether this

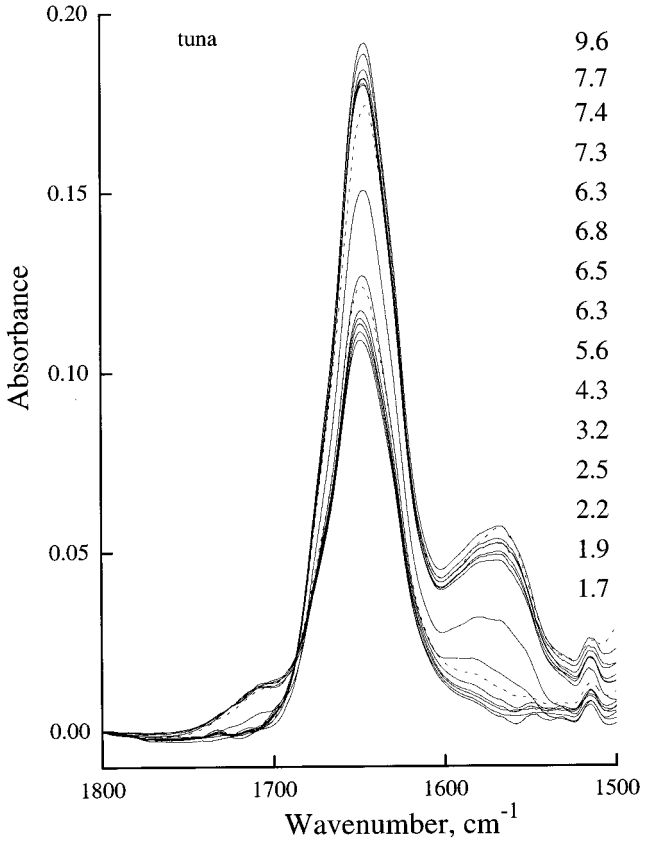

FIGURE 10: pD dependence of 4 mM tuna cyt *c* in 20 mM $NaPO_4$ and D_2O. The pDs are indicated on the figure, with the sequence being in order of intensity at ~1565 cm^{-1}. For clarity, the spectra at pD 4.3 and 9.6 are shown as dotted lines.

has an effect on ν^{a}_{OCO}, which arises from carboxylates on the surface. At neutral pH, however, there is little difference in the carboxylate stretching region of the oxidized and reduced cytochromes (Figure 6). But when the pH extremes are considered, spectral differences begin to emerge between the two redox states. Redox changes have been shown to affect the stability of cyt *c* (Bhuyan et al., 1991), and they should be detectable by monitoring the amide I′ and carboxylate stretches at low pH and low ionic strength. Therefore, caution must be exercised in attributing these observed differences solely to the change in oxidation state: we have to consider also that the rather large observed changes are due to changes in the stability and the folding of the protein resulting from lowering the pH.

Protonation of the Heme Propionic Acids. The protonation state of the propionic acids of the heme group should affect the redox chemistry, since electrostatic calculations have recently shown that protonation affects the field across the porphyrin tetracycle (Köhler et al., 1996). It is therefore of interest to know if they are protonated. The X-ray structure of horse cyt *c* (Bushnell et al., 1990) shows that only four atoms of the heme (corresponding to the carbon atoms of one pyrrole) are exposed to solvent but that the propionate groups are deeply buried and not exposed to external solvent. There is yet to be agreement in the literature concerning their pK_a: some studies report them undissociated at neutral pH (Koppenol & Margoliash, 1982) and others fully ionized (Brems & Stellwagen, 1983). Tonge and co-workers (Tonge et al., 1989) have suggested that one of the propionate groups may have an exceptionally high p*K* (>9) while proposing a value of <4.5 for the second one. Upon the basis of the data presented in Figure 1, a COOH group with a p*K* of 9 would have its $\nu_{C=O}$ at 1685 cm^{-1}, with absorption probably hidden to some extent in the amide I band. The spectra for yeast cyt *c* in H_2O (Figure 5), for horse cyt *c* (Figure 7) and for tuna cyt *c* in D_2O (Figure 10) show this region in the alkaline range. They all show no indication of any $\nu_{C=O}$ contribution whatsoever (which, if overlapped by the amide I and I′ bands, would manifest itself as spectral shifts as pD is changed). We therefore conclude that the propionic acids of the heme are ionized in all three cyt *c*s with a pK_a of <6.5. This compares well with the p*K* of the heme in MP-11 (~6) (Figure 3) and is consistent with a calculated value of 5.7 for a model porphyrin with fully ionized propionic acids (Falk, 1975).

In summary, the major conclusion of this paper is that the carboxylate antisymmetric vibrations in cyt *c* show a variety of vibrational frequencies which can be clearly observed in the IR spectrum of cyt *c*. The shifts of ν^{a}_{OCO} with p*K* for model compounds, the broadness of the band in the protein, and its pD dependence suggest that carboxyls on the surface of cyt *c* experience a variety of environments, which can arise from the presence of different local electric fields and as a result of hydrogen bonding.

ACKNOWLEDGMENT

The authors thank Dr. Chris Moser for helpful discussions and C. W. Vanderkooi for help in data analysis.

REFERENCES

Alben, J. O. (1978) in *The Porphyrins* (Dolphin, D., Ed.) pp 323−345, Academic Press, Inc., NY.

Augspurger, J. D., Dykstra, C. E., & Oldfield, E. (1991) *J. Am. Chem. Soc. 113*, 2447−2451.

Bandekar, J. (1992) *Biochim. Biophys. Acta 1120*, 123−143.

Bellamy, L. J. (1980) *The Infrared Spectra of Complex Molecules 2*, Chapman and Hall, London.

Bhuyan, A. K., Elöve, G. A., & Roder, H. (1991) *J. Cell. Biochem. 15*G, 188.

Brems, D. N., & Stellwagen, E. (1983) *J. Biol. Chem. 258*, 3655−3660.

Bushnell, G. W., Louie, G. V., & Brayer, G. D. (1990) *J. Mol. Biol. 214*, 585−595.

Chirgadze, Y. N., Fedorov, O. V., & Trushina, N. P. (1975) *Biopolymers 14*, 679−694.

Davoodi, J., Wakarchuk, W. W., Campbell, R. L., Carey, P. R., & Surewicz, W. K. (1995) *Eur. J. Biochem. 232*, 839−843.

Diem, M. (1993) *Introduction to Modern Vibrational Spectroscopy*, John Wiley & Sons, New York.

Dunn, G. E., & McDonald, R. S. (1969) *Can. J. Chem. 47*, 4577−4588.

Dwivedi, A. M., & Krimm, S. (1984) *Biopolymers 23*, 923−943.

Falk, J. E. (1975) *Porphyrins and Metalloporphyrins*, Elsevier, Amsterdam.

Goormaghtigh, E., Cabiaux, V., & Ruysschaert, J.-M. (1994) *Subcell. Biochem. 23*, 329−362.

Goto, Y., Calciano, L. J., & Fink, A. L. (1990a) *Proc. Natl. Acad. Sci. U.S.A. 87*, 573−577.

Goto, Y., Takahashi, N., & Fink, A. L. (1990b) *Biochemistry 29*, 3480−3488.

Goulden, J. D. S. (1954) *Spectrochim. Acta 6*, 129−133.

Gupta, R. K., & Koening, S. H. (1971) *Biochem. Biophys. Res. Commun. 45*, 1134−1143.

Heimburg, T., & Marsh, D. (1993) *Biophys. J. 65*, 2408−2417.

Jeng, M.-F., & Englander, S. W. (1991) *J. Mol. Biol. 221*, 1045−1061.

Jeng, M.-F., Englander, S. W., Elove, G. A., Wand, A. J., & Roder, H. (1990) *Biochemistry 29*, 10433−10437.

Kitagawa, T., & Ozaki, Y. (1987) in *Metal Complexes with Tetrapyrrole Ligands, I.* (Buckler, J. W., Ed.) pp 73−114, Springer, New York.
Koeppe, R. E., II, & Stroud, R. M. (1976) *Biochemistry 15*, 3450−3458.
Köhler, M., Gafert, J., Friedrich, J., Vanderkooi, J. M., & Laberge, M. (1996) *Biophys. J. 71*, 77−85.
Koppenol, W. H., & Margoliash, E. (1982) *J. Biol. Chem. 257*, 4426−4437.
Koyama, Y., Umemoto, Y., Akamatsu, A., Uehara, K., & Tanaka, M. (1986) *J. Mol. Struct. 146*, 273−287.
Krawczyk, S. (1989) *Biochim. Biophys. Acta 976*, 140−149.
Krimm, S., & Bandekar, J. (1986) *Adv. Protein Chem. 38*, 181−364.
Kushkuley, B., & Stavrov, S. S. (1996) *Biophys. J. 70*, 1214−1229.
Leitch, F. A., Moore, G. R., & Pettigrew, G. W. (1984) *Biochemistry 23*, 1831−8.
Lin-Vien, D., Colthup, N. B., Fateley, W. G., & Grasselli, J. G. (1991) *The Handbook of Infrared and Raman Characteristic Frequencies of Organic Molecules* , Academic Press, San Diego.
Liptay, W. (1974) in *Excited States* (Lim, E. C., Ed.) pp 129−229, Academic Press, New York.
Louie, G. V., & Brayer, G. D. (1990) *J. Mol. Biol. 214*, 527−555.
Matthew, J. B., Weber, P. C., Salemme, F. R., & Richard, F. M. (1983) *Nature (London) 301*, 169−171.
Moore, G. R., Pettigrew, G. W., Pitt, R. C., & Williams, R. J. (1980) *Biochim. Biophys. Acta. 590*, 261−71.
Morishima, I., Ogawa, S., Yonezawa, T., & Iizuka, T. (1977) *Biochim. Biophys. Acta 495*, 287−298.
Myer, Y. P. (1968) *Biochemistry 7*, 765−776.
Myer, Y. P., & Saturno, A. F. (1991) *J. Protein Chem. 10*, 481−494.
Northrup, S. H., Boles, J. O., & Reynolds, J. C. L. (1987) *J. Phys. Chem. 91*, 5991−5998.
Northrup, S. H., Boles, J. O., & Reynolds, J. C. L. (1988) *Science 241*, 67−70.
Northrup, S. H., Wensel, T. G., Meares, C. F., Wendoloski, J. J., & Matthew, J. B. (1990) *Proc. Natl. Acad. Sci. U.S.A. 87*, 9503−9507.
Ogoshi, H., Saito, Y., & Nakamoto, K. (1972) *J. Chem. Phys. 57*, 4194−4202.
Park, K. D., Guo, K., Adebodun, F., Chiu, M. L., Sligar, S. G., & Oldfield, E. (1991) *Biochemistry 30*, 2333−2347.
Rogers, N. K., Moore, G. R., & Sternberg, M. J. (1985) *J. Mol. Biol. 182*, 613−616.
Simonson, T., & Perahia, D. (1995) *Proc. Natl. Acad. Sci. U.S.A. 92*, 1082−1086.
Tiede, D. M., Vashishta, A.-C., & Gunner, M. R. (1993) *Biochemistry 32*, 4515−4531.
Tonge, P., Moore, G. R., & Wharton, C. W. (1989) *Biochem. J. 258*, 599−605.
Vanderkooi, J. M., & Erecinska, M. (1974) *Arch. Biochem. Biophys. 162*, 385−391.
Vanderkooi, J. M., Erecinska, M., & Chance, B. (1973) *Arch. Biochem. Biophys. 154*, 219−229.
Weast, R. C., & Astle, M. M. (1982−1983) *CRC Handbook of Chemistry and Physics*, CRC Press, Inc., Boca Raton, FL.
Wilson, M. T., & Ranson, R. J. (1977) *Eur. J. Biochem. 77*, 193−199.
Wright, W. W., & Vanderkooi, J. M. (1997) *Biospectroscopy 3*, 457−467.

BI971559N